

Assessing the control of finite-amplitude instabilities via a probabilistic protocol

Application to transitional flows



LEVERHULME
TRUST

C. Beaume¹, A. Pershin², S. M. Tobias¹

¹ School of Mathematics, University of Leeds, Leeds LS2 9JT, UK

² Department of Physics, University of Oxford, Oxford OX1 3PU, UK



Motivation

Finite-amplitude instabilities may arise in systems featuring multi-stability. Characterizing the boundary between the basins of attraction of the stable states represents invaluable information to understand and control these instabilities. Unfortunately, in large-dimensional systems, the structure of this boundary is rarely trivial which makes an exhaustive characterization virtually impossible.

We consider an example of such a system: plane Couette flow, the three-dimensional viscous flow confined between two parallel, no-slip walls moving in opposite directions. The fluid satisfies the Navier–Stokes equation and the incompressibility constraint:

$$\frac{\partial \mathbf{u}}{\partial t} + (\mathbf{u} \cdot \nabla) \mathbf{u} = -\nabla p + \frac{1}{Re} \nabla^2 \mathbf{u}, \quad (1)$$

$$\nabla \cdot \mathbf{u} = 0, \quad (2)$$

where \mathbf{u} is the velocity field, t is the time, p is the pressure and Re is the Reynolds number, which expresses the ratio between inertial and viscous forces within the fluid. These equations are complemented with no-slip boundary conditions in the wall-normal direction:

$$\mathbf{u} = y\mathbf{e}_x, \quad \text{at} \quad y = \pm 1, \quad (3)$$

as well as periodic boundary conditions in the streamwise (x) and spanwise (z) directions. This flow admits a stable solution, the laminar flow $\mathbf{u}_{lam} = y\mathbf{e}_x$, which is prone to a finite-amplitude instability, transition to turbulence (see Figure 1).

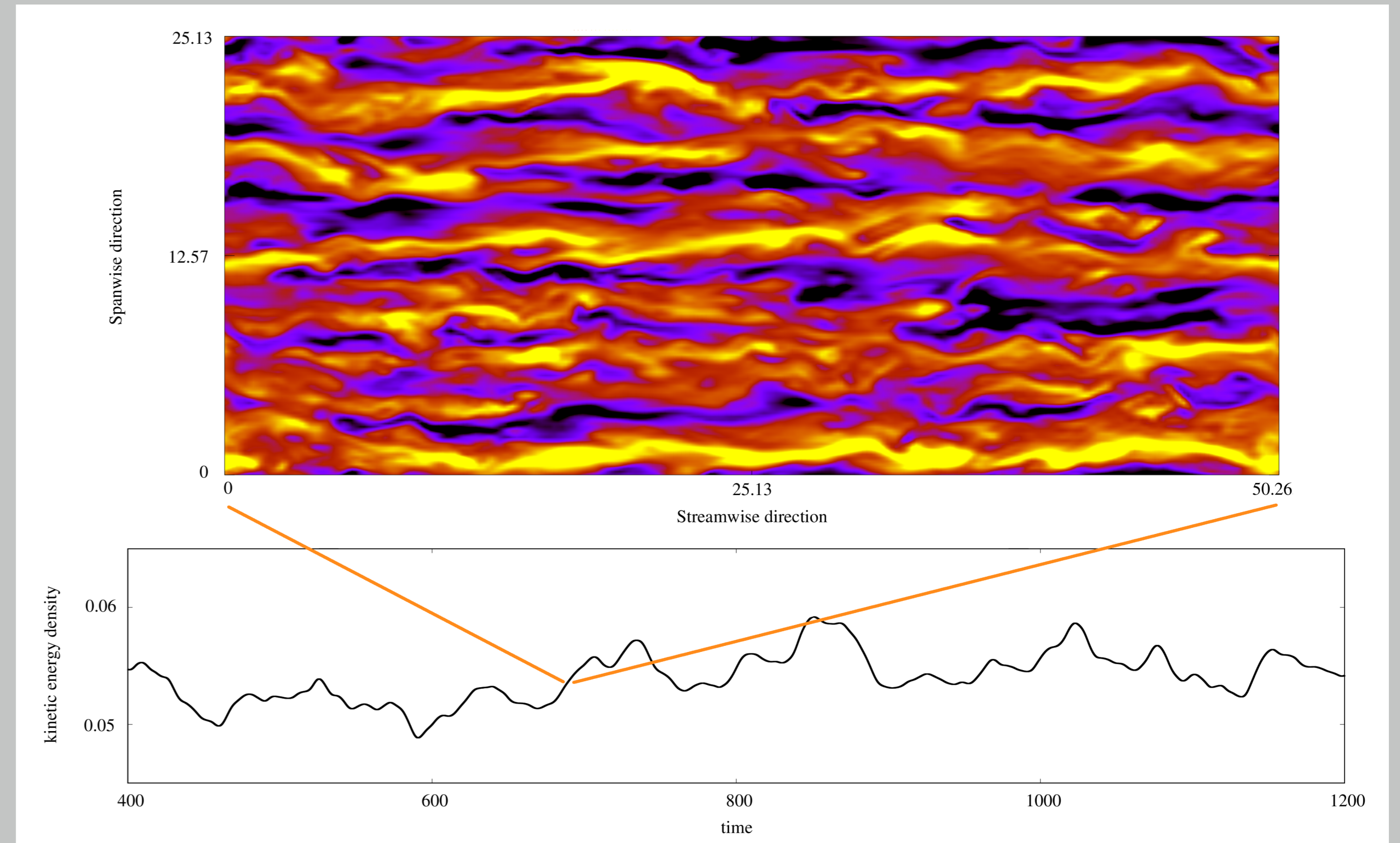


Figure 1: Example of turbulent flow in a large domain ($L_x = 16\pi$, $L_z = 8\pi$) for $Re = 500$ showing the chaotic oscillations of the kinetic energy density as a function of time as well as a mid-plane ($y = 0$) contour plot of the streamwise (x -)velocity, where black (resp. yellow) denotes values inferior to -0.3 (resp. superior to 0.3).

Probabilistic protocol

Methodology

To study the robustness of the laminar flow, we perturb it and compute the probability of the perturbation decaying, known as the laminarization probability, as a function of the perturbation kinetic energy [1].

For a set kinetic energy density E , initial conditions,

$$\mathbf{u}_{init} = (1 + B)\mathbf{u}_{lam} + A\mathbf{u}_\perp, \quad (4)$$

where the random perturbations, $A\mathbf{u}_\perp + B\mathbf{u}_{lam}$, are generated in the following way:

- Generate \mathbf{u}_\perp : spectral coefficients are drawn from uniform distributions with support size decaying exponentially with the wavenumber magnitude; ensure incompressibility; normalize.
- Generate B : draw from the uniform distribution in $[-2E/|\mathbf{u}_{lam}|; 2E/|\mathbf{u}_{lam}|]$.
- Compute A : $A = \pm\sqrt{2E - B^2|\mathbf{u}_{lam}|}$, where the sign is chosen randomly.
- Finalize: time-integrate the resulting field for a small time to ensure boundary conditions without impacting energy much.

Benchmark case

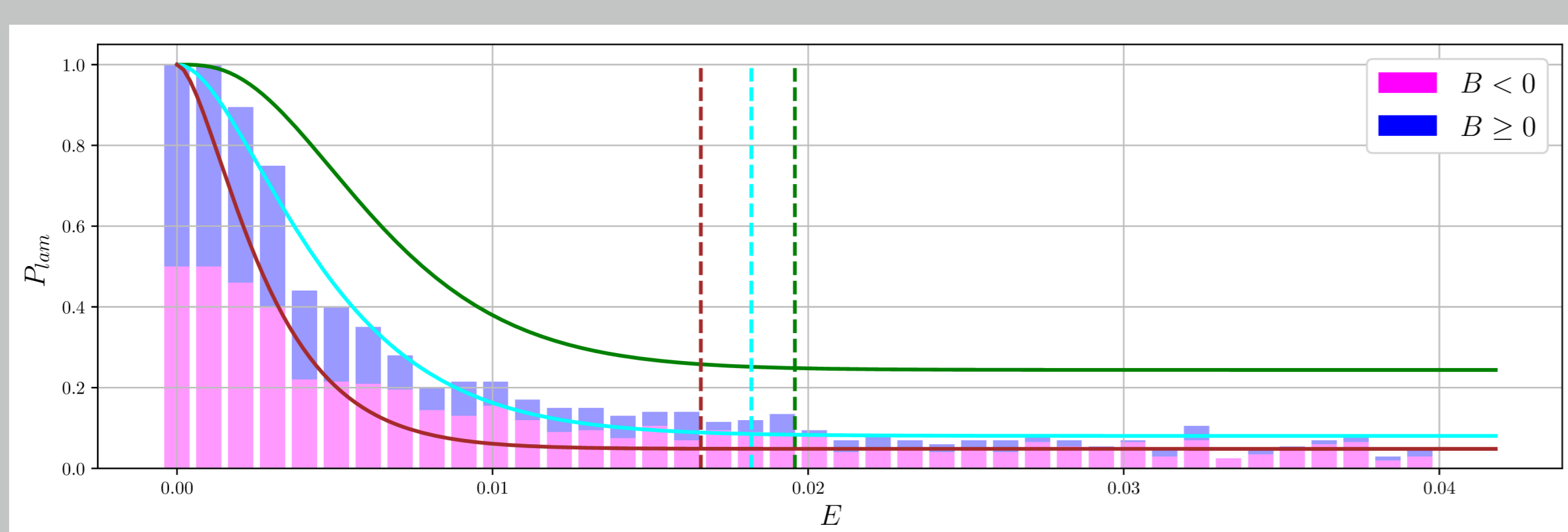


Figure 2: Laminarization probability P_{lam} as a function of the perturbation kinetic energy E for $Re = 500$ in a small domain ($L_x = 4\pi$, $L_z = 32\pi/15$). The bars represent the numerical results, where the pink (resp. blue) components indicate the contribution from the reduced (resp. enhanced) bulk shear perturbations. The cyan curve represents the fit to a cumulative distribution function for the gamma distribution [1]. The edge state (attractor along the separatrix between the basin of attraction of the laminar flow and that of turbulence) is a steady state and its energy is indicated using the cyan vertical dashed lines. Results for $Re = 400$ (resp. $Re = 700$) are shown using green (resp. red) lines.

⇒ The laminarization probability decreases with increasing perturbation energy and with increasing Re .

⇒ The edge of chaos energy does not look like a good descriptor of the laminar flow robustness.

⇒ The energy of the minimal seed (lowest energy perturbation that does not laminarize) is too small to be of practical relevance.

Example of control

Control strategy

We aim to control the flow using wall oscillations in the spanwise direction [2]. The non-periodic boundary condition is modified into:

$$\mathbf{u} = y\mathbf{e}_x + W_{osc} \sin(\omega t + \phi)\mathbf{e}_z, \quad \text{at} \quad y = \pm 1, \quad (5)$$

where the oscillations are characterized by their magnitude W_{osc} , their frequency ω and their phase ϕ . The methodology is that presented in the left column with a suitably modified \mathbf{u}_{lam} . The choice of the phase ϕ did not impact results.

Results

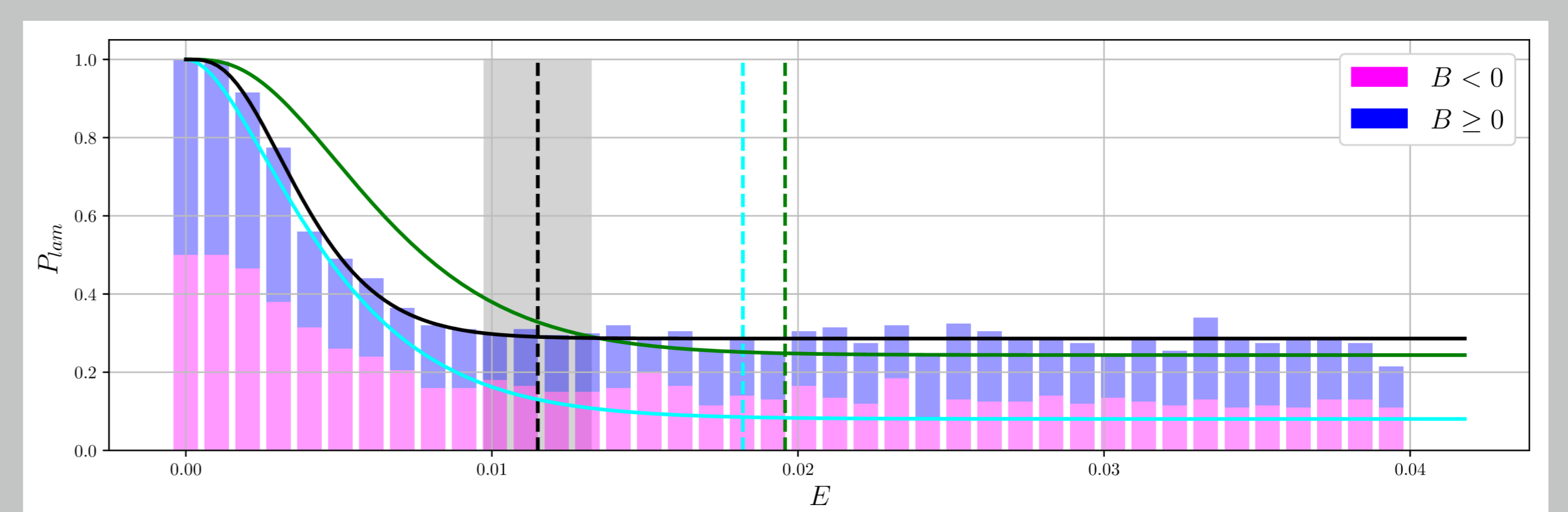


Figure 3: Same as Figure 2 but for $W = 0.3$ and $\omega = 1/16$. Here, the attractor along the edge of chaos is chaotic and its average energy is represented in the vertical black dashed line with the shaded region around it indicating a span of two standard deviations around the average value. The green and the cyan lines are the same as in Figure 2.

⇒ “Large” amplitude perturbations are the most efficiently controlled.

⇒ Control acts mainly on enhanced bulk shear perturbations.

⇒ Evolution of the edge of chaos energy misleading.

To quantify control efficiency, we introduce the laminarization score [3]:

$$S = \int_0^{E_{max}} p_{lam}(E) f_E(E) dE, \quad (6)$$

where the laminarization probability p_{lam} is weighed by f_E to put more emphasis on the more easily generated, low-energy perturbations, and where E_{max} is the maximum perturbation energy deemed relevant. Results in Figure 4 are shown for:

$$f_E(E) = \frac{E_{avg}^{-1} \exp(-E/E_{avg})}{1 - \exp(-E_{max}/E_{avg})}. \quad (7)$$

⇒ Best control is obtained for oscillation frequency $\omega \approx 1/8$.

⇒ Increasing the oscillation amplitude improves the robustness of the laminar flow.

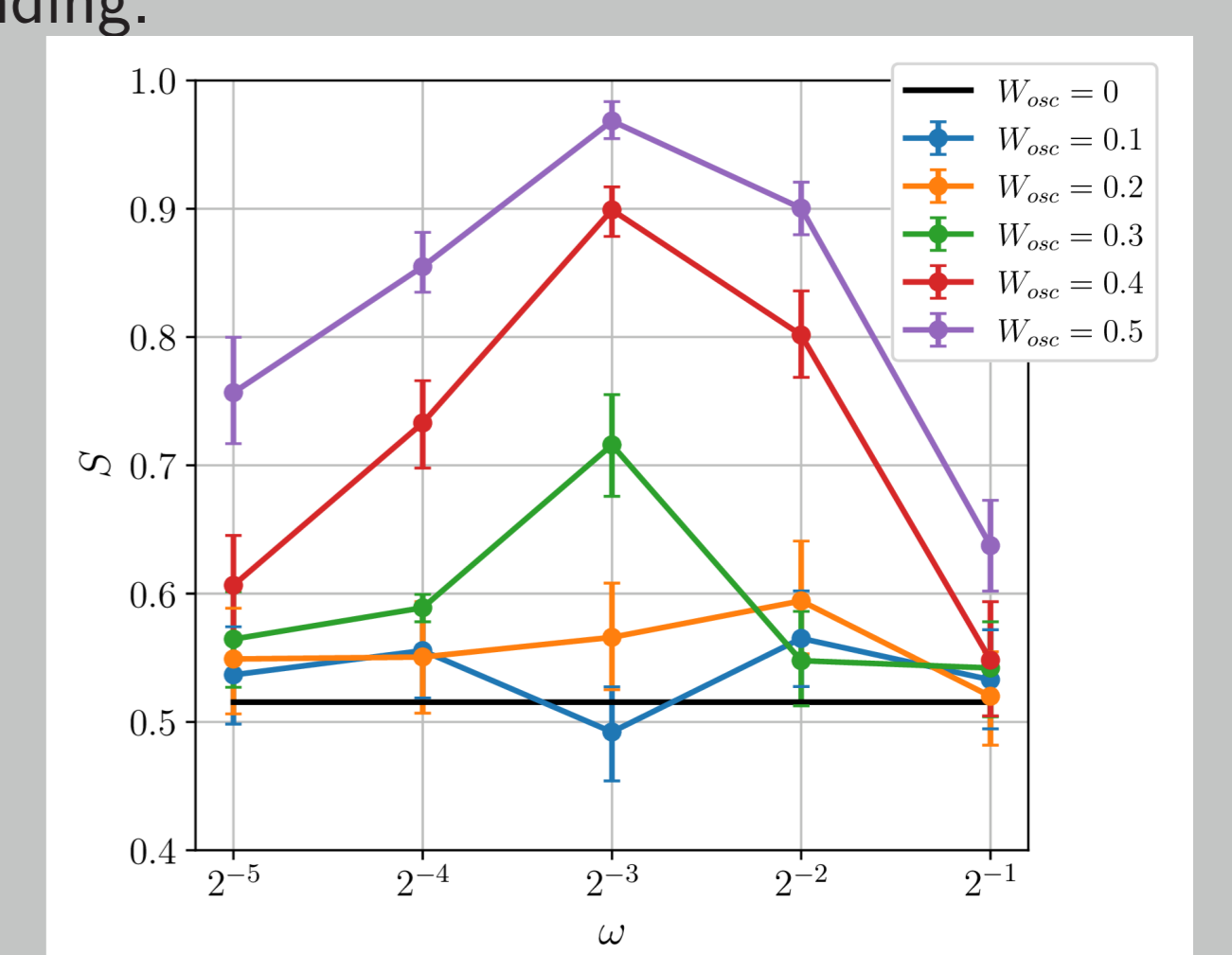


Figure 4: Laminarization score S as a function of the control frequency ω and amplitude W_{osc} . Error bars represent uncertainty.

Contact

C. Beaume: c.m.l.beaume@leeds.ac.uk
A. Pershin: anton.pershin@physics.ox.ac.uk
S. M. Tobias: s.m.tobias@leeds.ac.uk

References

- [1] A. Pershin, C. Beaume & S. M. Tobias, *J. Fluid Mech.* **895**, A16 (2020)
- [2] S. M. E. Rabin, C. P. Caulfield & R. R. Kerswell, *J. Fluid Mech.* **738**, R1 (2014)
- [3] A. Pershin, C. Beaume & S. M. Tobias, *in preparation* (2021)

Acknowledgments

CB acknowledges support from the Leverhulme Trust under Grant RPG-2018-311.